Development/Plasticity/Repair

Characterization of Rhythmic Ca^{2+} Transients in Early Embryonic Chick Motoneurons: Ca^{2+} Sources and Effects of Altered Activation of Transmitter Receptors

Sheng Wang,[1] Luis Polo-Parada,[2] and Lynn T. Landmesser[1]

[1]Department of Neurosciences, Case Western Reserve University, School of Medicine, Cleveland, Ohio 44106-4975, and [2]Dalton Cardiovascular Research Center, University of Missouri, Columbia, Missouri 65211

In the nervous system, spontaneous Ca^{2+} transients play important roles in many developmental processes. We previously found that altering the frequency of electrically recorded rhythmic spontaneous bursting episodes in embryonic chick spinal cords differentially perturbed the two main pathfinding decisions made by motoneurons, dorsal–ventral and pool-specific, depending on the sign of the frequency alteration. Here, we characterized the Ca^{2+} transients associated with these bursts and showed that at early stages while motoneurons are still migrating and extending axons to the base of the limb bud, they display spontaneous, highly rhythmic, and synchronized Ca^{2+} transients. Some precursor cells in the ependymal layer displayed similar transients. T-type Ca^{2+} channels and a persistent Na^{+} current were essential to initiate spontaneous bursts and associated transients. However, subsequent propagation of activity throughout the cord resulted from network-driven chemical transmission mediated presynaptically by Ca^{2+} entry through N-type Ca^{2+} channels and postsynaptically by acetylcholine acting on nicotinic receptors. The increased $[Ca^{2+}]_i$ during transients depended primarily on L-type and T-type channels with a modest contribution from TRP (transient receptor potential) channels and ryanodine-sensitive internal stores. Significantly, the drugs used previously to produce pathfinding errors altered transient frequency but not duration or amplitude. These observations imply that different transient frequencies may differentially modulate motoneuron pathfinding. However, the duration of the Ca^{2+} transients differed significantly between pools, potentially enabling additional distinct pool-specific downstream signaling. Many early events in spinal motor circuit formation are thus potentially sensitive to the rhythmic Ca^{2+} transients we have characterized and to any drugs that perturb them.

Introduction

Spontaneous and relatively synchronous bursting activity occurs in many developing neural circuits (for review, see Moody and Bosma, 2005). Is such activity simply an epiphenomenon that is produced as circuits begin to assemble and become active, or does it play an essential role in circuit formation? In the visual system, rhythmic waves of retinal activity are important for refining visual projections in multiple central targets (Stellwagen and Shatz, 2002; McLaughlin et al., 2003; Cang et al., 2005; Chandrasekaran et al., 2005). Spinal cords of chick and rodent embryos also exhibit rhythmic waves of propagating activity at early stages [embryonic day 12.5 (E12.5) mouse; E3.5–E5 chick] when motoneurons are still migrating and extending axons (Nishimaru et al., 1996; Milner and Landmesser, 1999; Branchereau et al., 2000; Hanson and Landmesser, 2004). However, this early activity differs from that characterized later in development (Sernagor et al., 1995). Rather than glutamatergic interneurons, the motoneurons themselves provide the main excitatory drive. This is achieved by the release of acetylcholine, which activates nicotinic receptors. GABA and glycine, which are both excitatory at this stage, also contribute to the excitatory drive (Milner and Landmesser, 1999; Hanson and Landmesser, 2003, 2004, 2006).

In ovo drug application was recently used to alter the frequency of this rhythmic activity during chick motor axon outgrowth. A modest decrease in frequency caused by the $GABA_A$ receptor antagonist picrotoxin, resulted in dorsal–ventral (D–V) pathfinding errors and a reduction in the expression of several molecules required for this guidance decision (Hanson and Landmesser, 2004). In contrast, a modest increase in frequency caused by the glycine uptake inhibitor sarcosine did not alter D–V pathfinding or guidance molecule expression but completely disrupted the subsequent pool-specific pathfinding decision (Hanson and Landmesser, 2006). These results suggest that the precise frequency of the spontaneous bursts is a critical variable. Such depolarizing bursts would be expected to cause Ca^{2+} transients in the motoneuron somas and growth cones. However, within the spinal cord, many transmitters, including acetylcholine (ACh), GABA, and glycine, will also be released during bursting episodes. These transmitters, acting via multiple receptor

Received Aug. 5, 2009; revised Sept. 25, 2009; accepted Oct. 26, 2009.

This work was supported by National Institutes of Health Grant NS19640 from National Institute of Neurological Disorders and Stroke. We thank Maryanne Pendergast and Ben Strowbridge for their help with the two-photon confocal imaging and gratefully acknowledge the use of the Neurosciences Imaging Center. We especially thank Michael O'Donovan and George Mentis for their initial instruction in two-photon Ca^{2+} imaging in isolated chick cords and M. Gartz Hanson for participating in these experiments. We also thank Diana Kunze, William Schilling, Yuka Maeno-Hikichi, Ksenia Kastanenka, and Stefan Herlitze for their comments on this manuscript.

Correspondence should be addressed to Lynn T. Landmesser, Department of Neurosciences, Case Western Reserve University, 10900 Euclid Avenue, Cleveland, OH 44106-4975. E-mail: lynn.landmesser@case.edu.

DOI:10.1523/JNEUROSCI.3809-09.2009

 0270-6474/09/2915232-13$15.00/0

subtypes, could affect directly or indirectly the Ca^{2+} transients. Strong, spaced depolarizations can be highly effective in modulating gene activity (Dolmetsch et al., 1997; Wu et al., 2001), and the frequency, amplitude, and path of entry of the ensuing Ca^{2+} transients can determine which genes or signaling pathways are activated (Watt et al., 2000; Moody and Bosma, 2005; Greer and Greenberg, 2008).

We therefore characterized spontaneous Ca^{2+} transients in chick motoneurons during this early period under control conditions and after blockade of specific transmitter receptors, Ca^{2+} channel subtypes, or the release of Ca^{2+} from internal stores. We found that recently generated motoneurons near the ependymal layer exhibited network-driven Ca^{2+} transients even before completing their migration to pool-specific locations. We also discovered novel roles of different Ca^{2+} channel subtypes and a persistent Na^{+} current in the actual generation of spontaneous rhythmic bursting activity. Therefore, any maternally taken drugs that alter these transients could potentially affect a number of early developmental processes.

Materials and Methods

In vitro *spinal cord preparation.* Experiments were performed on White Leghorn chick embryos at stage 25 (St 25) of Hamburger and Hamilton unless indicated otherwise. The preparation was made as described previously (Milner and Landmesser, 1999). Briefly, embryos were decapitated, eviscerated, and dissected in cool continuously oxygenated Tyrode's solution. A ventral laminectomy was performed to expose the spinal cord and muscle nerves and spinal nerves were exposed. After dissection, superfusion at a flow rate of 5 ml/min was performed continuously with oxygenated (95% O_2 and 5% CO_2) Tyrode's solution warmed to 30 ± 0.5°C.

Electrical recordings. Extracellular recordings were made using suction electrodes pulled from polyethylene tubing (PE190). Spontaneous bursts of activity were recorded in a gap-free mode with AxoScope 9 (Molecular Devices). The signals were recorded with GRASS P15 amplifiers with a bandwidth of 30 Hz to 3 kHz, digitized (DigiData 1200 series), and recorded on the computer using AxoScope 9 (Molecular Devices). Cords and nerves were also stimulated as described by Hanson and Landmesser (2003).

Patch-clamp recordings were made in standard (ruptured membrane patch) whole-cell configuration at room temperature (22–24°C). Pipettes (0.8–2 MΩ) were pulled from N51A Glass (Garner Glass), coated with Sylgard (Dow Corning), and fire-polished. Access resistance averaged 1.48 ± 0.12 MΩ ($n = 4$) and 1.25 ± 0.05 MΩ ($n = 4$), and membrane capacitance averaged 7.32 ± 1.28 pF ($n = 4$) and 5.3 ± 1.9 pF ($n = 4$) for the femorotibialis and sartorius cells, respectively. Capacitative transients and series resistance were electronically compensated using an Axopatch 200B amplifier (Molecular Devices). Currents were activated, acquired, and leak-subtracted using a hyperpolarizing P/4 protocol under the control of pClamp 8.0 (Molecular Devices), running on a Pentium processor-based computer (Dell 200 Pro). Currents were four-pole Bessel-filtered at 5 kHz and digitized at 20 kHz. All values expressed are mean ± SEM.

Solution. The bathing solution was as follows: 150 mM tetraethylammonium (TEA)-Cl, 5–10 mM $BaCl_2$, 1 mM $MgCl_2$, 10 mM glucose, 10 mM HEPES, and 1 μM tetrodotoxin, pH 7.3 (TEAOH). The pipette solution contained the following (in mM): 90 *N*-methyl-(+)-glucamine (NMG)-Cl, 30 CsCl, 30 TEA-Cl, 5 EGTA-NMG, 10 HEPES, 4 $MgCl_2$, 4 creatine phosphate, 4 ATP-Na, leupeptine, creatine kinase, and 0.2 GTP, pH 7.2 (CsOH). We used pharmacological agents and voltage protocols to characterize the contribution of different Ca^{2+} channel subtypes (Rusin and Moises, 1995) by using whole-cell recording of cells exposed to the following cumulative sequence of agents: 5 μM nifedipine (to block L-type), 1 μM ω-conotoxin GVIA (to block N-type), 20 nM ω-agatoxin IVA (to block P-type), 5 μM ω-conotoxin MVIIC (to block N + P/Q type), 2 μM $LaCl_3$ (to block T-type (Mlinar and Enyeart, 1993), or 100 μM $NiCl_2$ (to block T-R type). Although ω-conotoxin MVIIC and $NiCl_2$ will block several types of Ca^{2+} channels, when applied in this cumulative sequence, sensitivity of the resistant current to these agents can be used to reveal Ca^{2+} channel subtypes. Furthermore, we did not find any difference between the proportion of the total current carried by T-type Ca^{2+} channels using La^{3+} or Ni^{2+} as the antagonist (Mlinar and Enyeart, 1993). Cells were depolarized from −120 to +20 mV in 10 mV steps.

Two-photon optical imaging. We used methods developed by O'Donovan et al. (2008) for Ca^{2+} imaging of motor circuits in isolated spinal cords of chick and mouse embryos. Cords were prepared as described for physiological recording. After being exposed, the nerve was pulled into a suction electrode filled with calcium green-1 dextran 3000 molecular weight (MW) (30 mM; 5–10 μl; Invitrogen) dissolved in the following solution (in mM: 10 NaCl, 130 K-gluconate, 10 HEPES, 1.1 EGTA, 0.1 $CaCl_2$, 1 $MgCl_2$, and 1 Na_2ATP).

After retrograde labeling, the cord was transferred to a recording chamber and continuously superfused with Tyrode's solution bubbled with 95% O_2 and 5% CO_2 at a flow rate of 5 ml/min. The solution was heated to 30 ± 0.5°C using an In-line Solution Heater (SH-27B; Harvard Apparatus). In some cases, we also labeled presumed precursor cells within the ependymal layer by pressure injection of Ca^{2+} green dextran into the central canal of isolated spinal cords in low Ca^{2+}/high Mg^{2+} Tyrode's (in mM: 0.2 $CaCl_2$ and 7 $MgCl_2$), followed by electroporation using square voltage pulses (25 V; 50 ms duration; five pulses; two times) delivered by an ECM 830 electroporation system (BTX; Harvard Apparatus).

Ca^{2+} transients from backlabeled cells were visualized with the Bio-Rad Radiance 2100MP multiphoton laser-scanning microscope attached to an Olympus fixed-stage upright microscope (BX51WI; Olympus) with a 40× water-immersion objective. Before two-photon optical imaging, labeled neurons were visualized by illumination supplied by a 150 W xenon bulb (1600 Power Supply; Opti Quip) and the focal plane for the subsequent laser scanning was chosen. The laser was tuned to 780 nm to excite the tissue and emission was collected at 530 nm wavelength. A timed series of images from a field of view that contained labeled neurons was acquired at a 16 bit resolution with scan time between 350 and 520 ms per frame. To determine the position within the cord of the labeled neurons from which data were acquired, a transmission detector was applied for bright-field transmission imaging allowing a transmission image to be acquired simultaneously with the confocal fluorescent images. The positions of labeled cells could be confirmed based on the merged images.

Data analysis of time-lapse images was made using MetaMorph7 (Molecular Devices). Background subtraction was performed before measuring fluorescence intensity, which could be in turn determined using this software. Normalized fluorescence changes were calculated as $\Delta F/F = (F_t - F_0)/(F_0)$, where F_t is the background-corrected average fluorescence signal within the measurement box at any time point and F_0 is the background-corrected average intensity at the resting level (i.e., between bursting episodes). In some cases, Ca^{2+} transients were evoked by electrically stimulating the cord as described above. For cords treated with ω-conotoxin GVIA, Ca^{2+} transients were evoked by direct depolarization via bath application of 100 mM KCl for 1 min. The amplitude and duration of the evoked Ca^{2+} transients were then measured before and after ω-conotoxin GVIA.

Immunohistochemistry. St 25 embryonic chick lumbar motoneurons were retrogradely labeled with Ca^{2+} green dextran as described above. The cord was then fixed in 3.7% formaldehyde, frozen, sectioned, and stained for Lim1/2 and Islet-1 transcription factors as described previously (Hanson and Landmesser, 2004) to identify LMCl motoneurons projecting to sartorius and femorotibialis muscles and LMCm motoneurons projecting to the adductor muscle.

Drug treatment of intact spinal cords and data analysis. All drugs were bath-applied for 15 min before assessing the effect on activity. Episode frequency was expressed as the interval between bursting episodes. At least 10 episodes of activity were measured for control and any drug treatment and expressed as the average. Each drug treatment was conducted in at least three spinal cords, and data were expressed as the mean ± SEM. To confirm that the effects were reversible, in the majority of cases, drugs were washed out until burst parameters returned to control levels.

A list of drugs used in our experiments includes the following: Ca^{2+} green-1 dextran 3000 MW; the nicotinic cholinergic receptor blockers, mecamylamine, dihydro-β-erythroidine hydrobromide (DHβE) and methyllycaconitine (MLA); the muscarinic cholinergic antagonist atro-

pine; the $GABA_A$ receptor blocker picrotoxin; $GABA_B$ receptor blocker saclofen; the inhibitor of the GlyT1 glycine transporter sarcosine; the persistent Na^+ current blocker riluzole; the L-type Ca^{2+} channel blocker nifedipine; the T-type Ca^{2+} channel blocker nickel chloride and La^{3+}; the P-type Ca^{2+} channel blocker ω-agatoxin IVA; the P/Q-type Ca^{2+} channel blocker ω-agatoxin TK; the N-type Ca^{2+} channel blocker ω-conotoxin GVIA; the N- and P/Q-type channel blocker ω-conotoxin MVIIC; the R-type Ca^{2+} channel blocker SNX-482; the Ca^{2+} internal store depleter cyclopiazonic acid (CPA); the ryanodine-sensitive Ca^{2+} store blocker ryanodine; the inositol-(1,4,5)-trisphosphate (IP_3)-sensitive Ca^{2+} store antagonist 2-aminoethoxydiphenyl borate (2-APB), the phospholipase C inhibitor 1-[6-([17β-methoxyestra-1,3,5(10)-trien-17-yl]amino)hexyl]-1*H*-pyrrole-2,5-dione (U73122); the transient receptor potential (TRP) channel blocker 1-2-(4-methoxyphenyl)-2-[3-(4-methoxyphenyl)propoxy] ethyl-1*H*-imidazole (SKF-96365). Ryanodine, SNX-482, and U73122 were purchased from BIOMOL, Ca^{2+} green-1 dextran (3000 MW) from Invitrogen, and all other drugs from Sigma-Aldrich.

All the data are displayed as mean ± SE. Statistical analysis was made using one-way ANOVA or two-tailed Student's *t* test. A probability of <0.05 was accepted as significant.

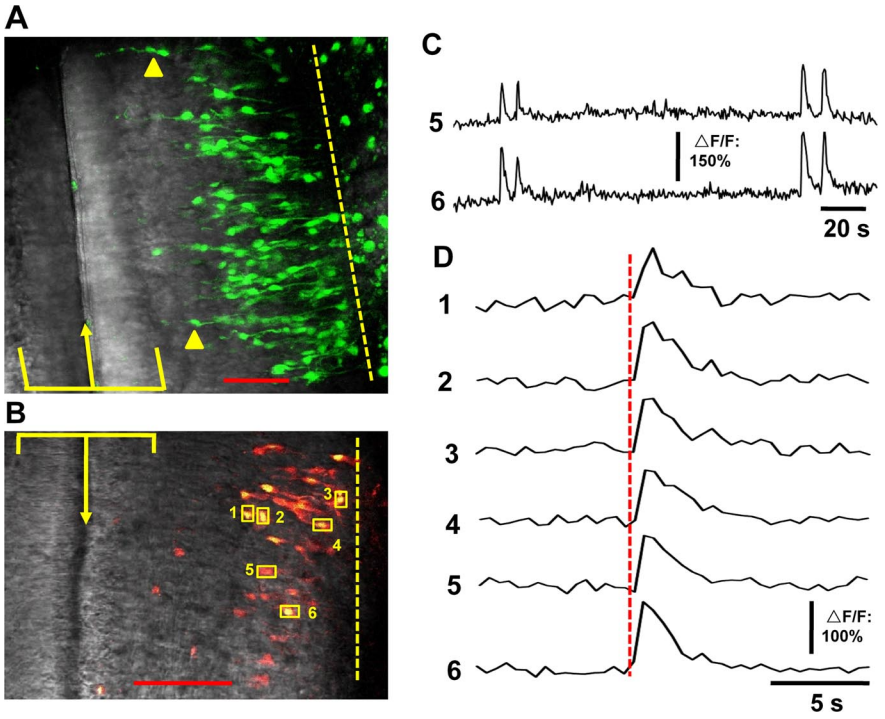

Figure 1. Embryonic chick motoneurons retrogradely labeled with Ca^{2+} green dextran exhibit rhythmic Ca^{2+} transients. ***A***, St 25 motoneurons retrogradely labeled from LS1 spinal nerve visualized from a stack of serial images at 1 μm steps between 50 and 87 μm below the ventral cord surface. The yellow bracket indicates the extent of the proliferative ependymal layer; arrow, the central canal; and dashed yellow line, the lateral extent of the spinal cord. Cells lateral to this boundary are dorsal root ganglion cells. Some motoneuron somas are located laterally in the LMC, but many others are medial and are still migrating, several (arrowheads) being close to the ependymal layer and retaining central processes. Scale bar, 50 μm. ***B***, Fluorescent neurons within a single focal plane and shown in pseudocolor were retrogradely labeled from spinal nerve L3. Scale bar, 60 μm. ***C***, Representative examples of two consecutive episodes of activity showing the Ca^{2+} transients of cells 5 and 6 in ***B***. Almost all cells in this focal plane, ~21, exhibited similar transients demonstrating relatively synchronized spontaneous rhythmic Ca^{2+} signals. ***D***, Single Ca^{2+} transients, shown on a faster timescale, recorded from cells 1–6 as indicated in ***B***. Cells close to (1) and farther from (3) the midline had transients of similar amplitude.

Results

Rhythmic Ca^{2+} transients occur in motoneurons that have not completed their migration to the lateral motor column (LMC) and these exhibit pool-specific differences in duration

By early St 25 (E4.5), many motoneurons in lumbar segments LS1–LS3 have projected axons to the crural plexus and have just made a binary dorsal–ventral pathfinding decision. Although muscles have not yet formed and motor axons are still growing toward their target regions, we were able to retrogradely label their somas by injecting Ca^{2+} green dextran into individual spinal nerves (Fig. 1). Retrograde labeling and Ca^{2+} imaging of chick motoneurons have been performed at later developmental stages (E8–E12) after they have migrated to their pool-specific locations, established peripheral synapses, and acquired pool-specific bursting patterns (for review, see O'Donovan et al., 2008). We have previously characterized the parameters of rhythmic spontaneous activity in much less mature cords (E4–E5) by suction electrode recordings from spinal nerves or pool-specific fascicles (Milner and Landmesser, 1999). Although these recordings show how the population of motor axons at the recording site are activated during spontaneous bursting episodes, they do not enable one to know how early motoneurons are activated as they withdraw from the cell cycle and migrate from the ependymal layer. They also do not reveal the patterns of activation compared with the spatial locations of the motoneuron somas or whether all motoneurons are activated during each bursting episode. In the present study, we observed that large numbers of retrogradely labeled motoneuron somas could be clearly visualized along with their early processes. Since these were labeled from spinal nerves (Fig. 1), they will include motoneurons from the various pools located at that segmental level. At LS1 these would be predominantly sartorius and adductor motoneurons, whereas labeling from LS2 would include these plus the femorotibialis pool (Hanson and Landmesser, 2006). The cells labeled were clearly motoneurons based on their projection of axons into the limb and by their expression of the appropriate transcription factors (i.e., islet-1 for adductor motoneurons and Lim-1 for sartorius and femorotibialis motoneurons) (Tsuchida et al., 1994).

Although motoneurons at this stage of development had projected to the proximal limb bud, most had not completed their migration to the lateral motor column (Fig. 1) and their somas were elongated along the medial–lateral axis. Some were close to the ependymal layer (Fig. 1*A*, arrowheads), and many maintained central processes projecting toward or to (Fig. 1*A*, top arrowhead) the ependymal layer. These are apparently relatively newly generated motoneurons. We have in fact observed that chick motoneurons appear to migrate by a process of somal translocation along their peripherally projecting axons (K. Kastanenka and L. T. Landmesser, unpublished observations). Other motoneurons had reached positions appropriate for their pool and had begun to extend dendritic processes.

At St 25, rhythmic episodes of bursting activity, occurring every 1–2 min, can be recorded from the motoneuron axons (Milner and Landmesser, 1999; Hanson and Landmesser, 2004). Such bursts are network-driven waves of activity that can arise anywhere within the cord (but see Momose-Sato et al., 2009) and that propagate at ~10 μm/ms. After a burst, the network exhibits a

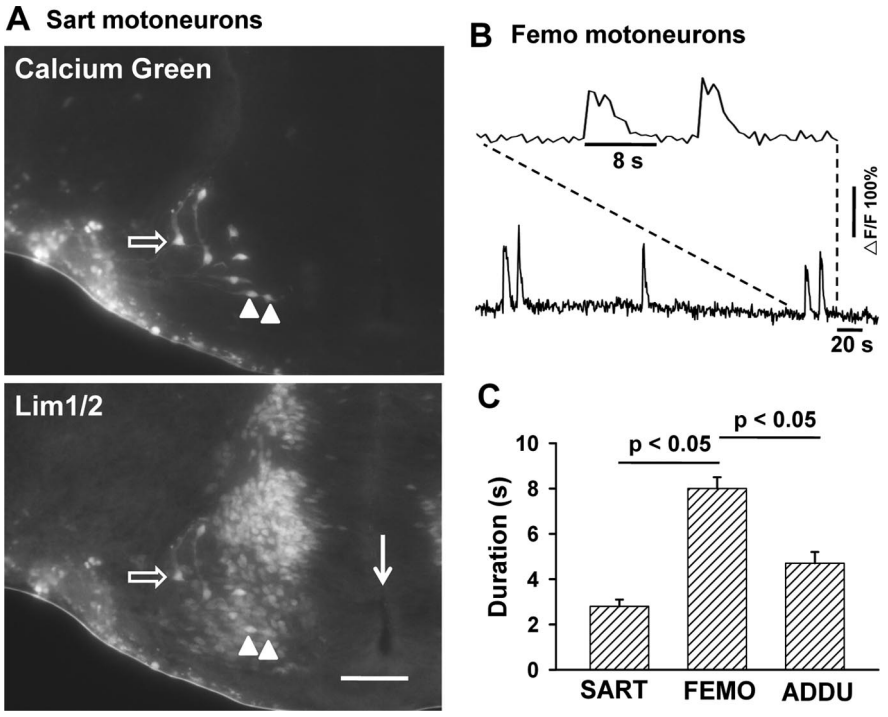

Figure 2. Early motoneuron pools exhibit pool-specific differences in Ca^{2+} transient duration. ***A***, Top, St 25 motoneurons retrogradely labeled from the sartorius nerve with calcium green dextran. Bottom, All these neurons stain strongly with an antibody that recognizes Lim1/2, characteristic of the sartorius pool. Some motoneurons (hollow white arrow) were located laterally in the sartorius pool position but other medially located cells (white triangles) were still migrating. Labeled neurons dorsal to the lateral motor column are interneurons that are positive for the Lim1/2 antibody. The white arrow indicates central canal. Ventral, Down; medial, right. Scale bar, 50 μm. ***B***, An example of spontaneous rhythmic Ca^{2+} transients recorded from a St 25 femorotibialis motoneuron. ***C***, Mean duration of Ca^{2+} transients from multiple embryos shows that they exhibit pool-specific differences. Error bars indicate SEM.

period of depression during which bursts cannot be evoked even by exogenous stimulation (Fedirchuk et al., 1999; Hanson and Landmesser, 2003). Recovery from this depression determines the intervals between episodes and thus their frequency. To characterize the Ca^{2+} transients associated with such bursts, two-photon Ca^{2+} imaging was performed in isolated cord preparations from groups of motoneurons within a single focal plane (Fig. 1*B*). Rhythmic Ca^{2+} transients occurred at 1–2 min intervals (Fig. 1*C*), as expected from the frequency of the electrical bursting episodes that drive them. At this developmental stage, each episode consists of one or two Ca^{2+} transients, reflecting the one or two bursts per episode. Within our fields of view, usually of a single spinal cord segment, most motoneurons were activated in a relatively synchronous manner. For example, the onset of the Ca^{2+} transients in cells 1–6 is shown on a faster time base in Figure 1*D*. Although the periods between episodes were long (1–2 min), the onset of the Ca^{2+} transients in each episode (compare with dashed line in Fig. 1*D*) differed by <500 ms, and thus can be considered to be synchronously activated.

Ca^{2+} transients were recorded from laterally located motoneurons that had completed their migration as well as from motoneurons located closer to the ependymal layer. Thus, soon after leaving the ependymal layer and while still undergoing somal migration, motoneuron somas are subject to rhythmic Ca^{2+} transients. To address whether the Ca^{2+} transients in the migrating cells might differ in amplitude from those that had completed migration, we measured these in cells located close to or farther from the ependymal layer. The mean peak intensity change ($\Delta F/F$) was 76 ± 11% (n = 10 cells) in motoneurons within 30–70 μm of the ependymal layer and 73 ± 7% (n = 10 cells) for motoneurons 80–130 μm from the ependymal layer. There were also no statistically significant differences in duration of the Ca^{2+} transients from these two groups (6.2 ± 0.4 s for laterally located motoneurons vs 5.9 ± 0.2 s for medially located motoneurons; n = 10 for each group) (also see, as an example, neurons 1 and 3 in Fig. 1*B*,*D*). Over the course of the experiments presented in Figures 1 and 2-5, we imaged motoneurons in all three segments that contribute to the crural plexus. Since these will include motoneurons belonging to different pools and we observed no statistically significant differences in the interepisode intervals of the spontaneous transients, whereas there were differences in duration (Fig. 2), we conclude that all motoneurons exhibit the same interepisode intervals and thus frequency of Ca^{2+} transients.

Although the segregation of axons into pool-specific fascicles is just beginning to occur, we have previously shown that it is possible to selectively record from the adductor, sartorius, and femorotibialis fascicles (Milner and Landmesser, 1999) and that they exhibit pool-specific differences in burst duration. To assess whether individual motoneuron pools might exhibit differences in either amplitude or duration of the Ca^{2+} transients, we retrogradely labeled motoneurons projecting to two dorsal muscles, the sartorius and femorotibialis, or to the ventral adductor muscles by sucking these fascicles into suction electrodes containing Ca^{2+} green dextran. To confirm the selectivity of our retrograde labeling, cords were subsequently frozen, cut transversely, and immunostained with antibodies that recognize the transcription factors Islet-1 and Lim-1. Motoneurons labeled from the sartorius nerve fascicle (Fig. 2*A*, top) all expressed high levels of Lim-1 (bottom), appropriate for this pool. Some of these neurons had migrated to the extreme lateral position of the sartorius pool (open arrow) while others (arrowheads) were still migrating. Motoneurons retrogradely labeled from both the sartorius and femorotibialis pools (LMC lateral motoneurons) were all Lim-1 positive and islet-1 negative, whereas the converse was true for those labeled from the obturator nerve (LMC medial motoneurons), as expected from previous studies (Tsuchida et al., 1994; Hanson and Landmesser, 2004). There are no pool-specific makers that are expressed this early in development. However, the appropriate segmental location of the pools, which differs between the sartorius and femorotibialis (Hanson and Landmesser 2006) was also observed in the present study.

The spontaneous Ca^{2+} transients recorded from a femorotibialis motoneuron are shown in Figure 2*B*. Clear differences were observed for the duration of the Ca^{2+} transients of the sartorius, femorotibialis, and adductor pools, respectively (Fig. 2*C*). Although the durations of the Ca^{2+} transients reflected the pool-specific differences in electrical burst duration, they were considerably longer. For example, the duration of bursts versus transients was 500 ms versus 2.5 s for the sartorius and 1–2 s

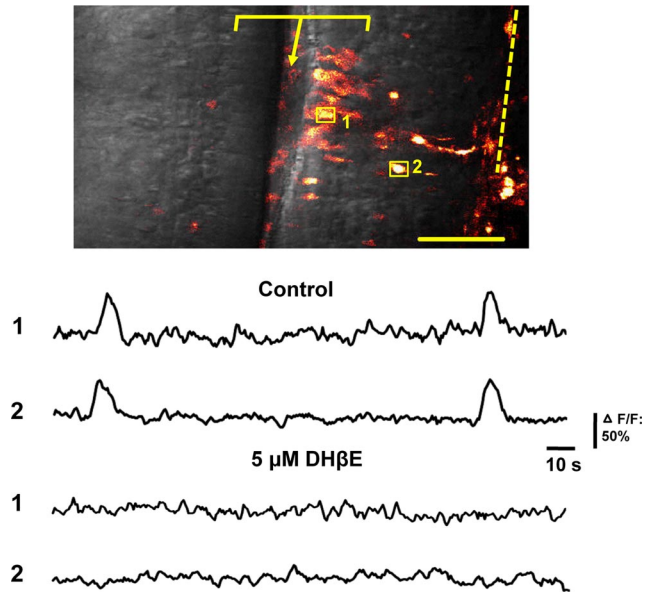

Figure 3. Rhythmic Ca^{2+} transients also occur in ependymal cells at lumbar cord levels. The top left panel shows many presumed precursor cells within the ependymal layer (indicated by the yellow bracket) were labeled by electroporation after injection of Ca^{2+} green dextran into the central canal. Some laterally located cells (motoneurons or interneurons) were also labeled. The arrow shows central canal/midline, and the dashed line shows the lateral boundary of the spinal cord. Trace 1 below (top) shows the Ca^{2+} transients recorded from cell 1 in the ependymal layer and trace 2 is from cell 2, a cell that has migrated from the ependymal layer and that may be either a motoneuron or an interneuron. Transients in both cells were approximately synchronous. The transients in both cells were blocked by the nicotinic antagonist DHβE at 5 μM (bottom pair of traces).

versus 8 s for the femorotibialis. In summary, these observations demonstrate early pool-specific differences in the duration of Ca^{2+} transients that could differentially affect downstream signaling pathways. However, despite these differences in duration, there were no statistically significant differences in the interepisode intervals of the Ca^{2+} transients from the three pools studied (121 ± 3, 119 ± 8, and 110 ± 10 s for sartorius, femorotibialis, and adductor pools, respectively; $p > 0.05$).

Rhythmic Ca^{2+} transients also occur in cells in the ependymal layer

Given that Ca^{2+} transients could be recorded in apparently newly generated motoneurons close to the ependymal layer, we assessed whether presumed precursor cells within the ependymal layer might also exhibit transients by introducing calcium green dextran into these cells using electroporation. We were able to label many cells within the ependymal layer as well as more laterally located neurons (Fig. 3, top panel). Ca^{2+} transients (bottom panel) occurred every 1–2 min in ependymal cells (Trace 1) and some of these were synchronous with those observed in neurons that had migrated out of the ependymal layer (trace 2). These ependymal cell Ca^{2+} transients appeared to be dependent on the neurally generated bursts as they were blocked by nicotinic antagonists such as DHβE that blocked spontaneous motoneuron bursts (Fig. 3, bottom pair of traces).

The effect of blocking different neurotransmitter receptors on spontaneous burst parameters

Our previous results demonstrated that D–V and pool-specific pathfinding decisions were highly sensitive to drug-induced alterations in the precise frequency of the bursting episodes. It was therefore important to determine whether these drugs, sarcosine and picrotoxin, also affected the frequency of the Ca^{2+} transients and to assess whether they might in addition alter their duration or amplitude. Therefore, two-photon Ca^{2+} imaging was performed in control and drug-treated St 25 isolated cord preparations. In addition, since ACh drives the bursting episodes at these early stages and can activate a variety of nicotinic and muscarinic receptors, we also characterized the effects of cholinergic antagonists on the Ca^{2+} transients.

We first confirmed (Fig. 4*A*) that the glycine uptake inhibitor sarcosine (500 μM) decreased and the $GABA_A$ antagonist picrotoxin (50 μM) increased the interval between bursting episodes as previously reported (Hanson and Landmesser, 2004, 2006). However, in addition, we show here that picrotoxin did not significantly alter burst amplitude, duration, or the number of bursts per episode (Fig. 4*A*). The $GABA_B$ antagonist saclofen also did not significantly affect any burst parameter (Fig. 4*A*). The α7 subunit-containing nicotinic receptors have a high permeability to Ca^{2+} (Bertrand et al., 1993; Séguéla et al., 1993) and are present in the LMC of embryonic chick spinal cords (Keiger et al., 2003). In addition, nicotinic signaling via these receptors regulates different aspects of neural development (Liu et al., 2006) including ACh-mediated growth cone retraction of cultured motoneurons (Pugh and Berg, 1994). However, we found that bath application of MLA, a specific antagonist of these receptors at 50 nM, had no effect on interepisode interval, burst duration, or amplitude and caused only a slight reduction in the number of bursts per episode (Fig. 4*A*). A broad antagonist of muscarinic receptors, atropine, was applied at 10 μM and also had no effect on any burst parameter (Fig. 4*A*).

Activation of non-α7 nicotinic receptors is required for the generation of spontaneous rhythmic activity in both chick (Milner and Landmesser, 1999) and mouse embryos (Hanson and Landmesser, 2003) and such activity can be transiently blocked by the antagonist DHβE. We first confirmed (Fig. 4*B*) that spontaneous activity could be transiently blocked by 5 μM DHβE ($n = 3$). Transient blockade also occurred in cords treated with 5 μM mecamylamine ($n = 3$) (data not shown), a noncompetitive nicotinic antagonist (Papke et al., 2008) that is more selective for $\alpha3\beta4$ subunits, and at lower doses of mecamylamine (0.5 and 1 μM; $n = 3$ for each) (data not shown) and DHβE (1 μM; $n = 3$) (data not shown), which should be selective for $\alpha3\beta4$ and $\alpha4\beta2$ subunit-containing receptors, respectively. Thus, both types of nicotinic receptors are normally required for generating spontaneous rhythmic activity at this developmental stage. However, a burst could still be elicited in the presence of these blockers by initiating a propagating burst by stimulation of thoracic cord (T2) or by direct stimulation of the lumbar cord at LS3 (Fig. 4*B*). Thus, the circuit driving bursting in the presence of non-α7 nicotinic blockers differs from that which normally drives the circuit. This fact will need to be considered when the effect of these nicotinic antagonists on Ca^{2+} transients or on downstream developmental processes is assessed.

The effect of blocking neurotransmitter receptors on spontaneous Ca^{2+} transients

Sarcosine and picrotoxin affected the frequency of the Ca^{2+} transients in the same way they had affected the frequency of spontaneous bursts; however, neither drug affected the duration or amplitude of the transients (Fig. 4*C*). Transient amplitude and duration were also not affected by blocking muscarinic receptors with atropine, α7 nicotinic receptors with MLA, or $GABA_B$ receptors with saclofen (Fig. 4*C*). Together, these results suggest that the

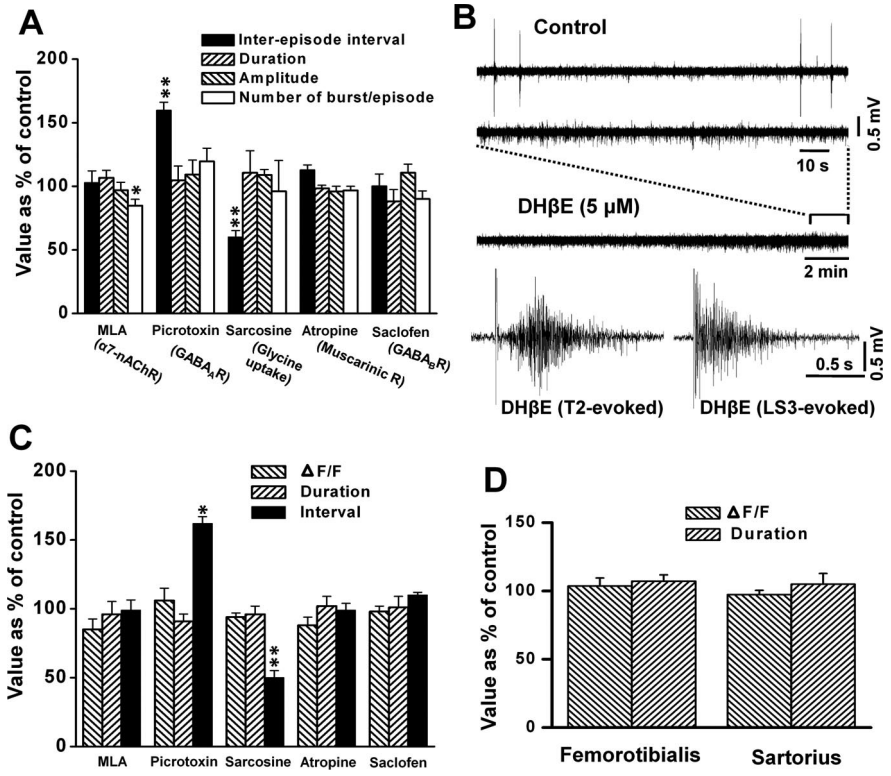

Figure 4. Effect of drugs that affect different neurotransmitters on burst parameters and Ca^{2+} transients. ***A***, Mean burst parameters expressed as percent of control after drug treatments. The data presented were mostly obtained from recordings from pool-specific fascicles and in a few cases from spinal nerves. In each individual case, we compared the burst parameters before and after the drug for each cell and expressed this as a percent of the before drug value. All pools were similarly affected by each treatment, and thus the data from all recordings were combined in this bar graph. MLA had only a slight effect on the number of bursts/episode ($p < 0.05$; $n = 5$). The $GABA_A$ receptor blocker picrotoxin (50 μM) increased and the glycine transporter inhibitor sarcosine (500 μM) decreased the mean interepisode interval ($p < 0.01$; $n = 6$ for picrotoxin and $n = 5$ for sarcosine). The muscarinic receptor blocker atropine (10 μM; $n = 5$) and the $GABA_B$ receptor blocker saclofen (50 μM; $n = 3$) were without effect on burst parameters. ***B***, The $\alpha4\beta2$ nAChR antagonist DHβE (5 μM) completely blocked the femorotibialis spontaneous bursts (top) but failed to inhibit bursts evoked by electrical stimulation at thoracic segment 2 (T2) or lumbosacral segment 3 (LS3). ***C***, Picrotoxin (50 μM) significantly decreased and sarcosine (500 μM) significantly increased the mean frequency of the Ca^{2+} transients ($p < 0.05$, $n = 9$ for picrotoxin; $p < 0.01$, $n = 6$ for sarcosine) but did not affect their amplitude or duration. The α-7 nicotinic receptor antagonist MLA (50 nM; $n = 11$), the muscarinic receptor antagonist atropine (10 μM; $n = 6$), and the $GABA_B$ receptor antagonist saclofen (50 μM; $n = 8$) had no effect on any of the Ca^{2+} transient parameters ($p > 0.05$ for all). As in ***A***, the Ca^{2+} transients were recorded both from individual pools and from unidentified motoneurons labeled from spinal nerves. Since pool-specific labeling is very difficult to obtain at this stage, more of the data in this bar graph were obtained after spinal nerve injection. However, since there were no observed differences in the effects of the drugs on Ca^{2+} transients recorded from identified or unidentified motoneurons, the data have been combined (for additional details, see Materials and Methods). ***D***, The effect of the nicotinic antagonist DHβE on evoked Ca^{2+} transients, during the period when the spontaneous transients were blocked. In the presence of 5 μM DHβE, Ca^{2+} transients could be evoked in femorotibialis ($n = 12$) and sartorius ($n = 7$) motoneurons by thoracic cord stimulation, and these did not differ significantly in amplitude or duration compared with control values. $^*p < 0.05$, $^{**}p < 0.01$, drug treatment compared with control. Error bars indicate SEM.

effects of chronic sarcosine or picrotoxin treatment on axon pathfinding were most likely attributable to alterations in the frequency of spontaneous bursts/Ca^{2+} transients, and not to alterations in their amplitude or duration. They also suggest that alterations in the activation of $GABA_A$ receptors, glycine receptors, $\alpha7$ nicotinic receptors, or muscarinic receptors probably did not contribute to the effects on pathfinding that we observed previously (Hanson and Landmesser, 2004, 2006). If they did contribute, the mechanism most likely did not involve the frequency, amplitude, or duration of the global somal Ca^{2+} transients. We also observed that 5 μM DHβE transiently blocked the spontaneous Ca^{2+} transients ($n = 13$ cells) (data not shown). However, during this period of blockade, Ca^{2+} transients with control level amplitudes could still be evoked by stimulation of the thoracic cord.

In initial experiments, in which motoneurons were labeled from spinal nerve LS3, evoked Ca^{2+} transients with normal amplitude and duration could be recorded in some cells but were completely blocked by DHβE in other cells. Similar results were obtained with mecamylamine. To determine whether the heterogenous responses to nicotinic blockers reflected differences in flexor versus extensor motoneurons, we next recorded from sartorius (flexor) and femorotibialis (extensor) motoneurons labeled from pool-specific fascicles. As shown in the bar graph (Fig. 4*D*), DHβE did not alter the amplitude or duration of the evoked Ca^{2+} transients in any of the motoneurons in either pool. Although we do not know the identity of the cells that were blocked by nicotinic antagonists, differential sensitivity to such antagonists does not represent a general difference between flexor and extensor motoneurons. In addition, we did not detect any heterogeneity in the response of cells within either pool. Additional studies will be needed to clarify the identity of the neurons, in which Ca^{2+} transients were blocked by non-$\alpha7$ nicotinic antagonists.

Effect of blocking Ca^{2+} channel subtypes on electrical burst parameters and associated Ca^{2+} transients

Ca^{2+} signaling modulates many neuronal processes (Bootman et al., 2001; Berridge et al., 2003; Clapham, 2007). Both the pattern of Ca^{2+} transients and the mode of Ca^{2+} entry can affect downstream signaling pathways (Moody and Bosma, 2005; Greer and Greenberg, 2008). We therefore sought to determine the sources of Ca^{2+} contributing to the early motoneuron Ca^{2+} transients via antagonists that affected specific Ca^{2+} channels or Ca^{2+} release from internal stores. However, the effect of such antagonists on the generation of spontaneous bursting activity itself had not been investigated, so this was studied first.

L-type Ca^{2+} channels increase in density on dissociated chick spinal cord motoneurons between E4 and E11 (McCobb et al., 1989), but it was not known whether they contributed to the generation or modulation of spontaneous bursting. We found that 10 μM nifedipine, an L-type Ca^{2+} channel blocker, did not alter the burst frequency ($p > 0.05$), although it had a slight effect on burst duration and amplitude ($p < 0.05$) (Fig. 5*A*). Clearly, acute blockade of L-type Ca^{2+} channels failed to abolish spontaneous bursts.

At mature mammalian neuromuscular junctions (Uchitel et al., 1992; Protti and Uchitel, 1993; Protti et al., 1996; Katz et al., 1997) and at synapses formed by E5–E7 chick motoneurons in culture (Hata et al., 2007), P/Q-type Ca^{2+} channels are almost exclusively responsible for synaptic vesicle exocytosis and transmitter release. To determine whether the propagation of sponta-

neous bursting activity within the spinal network at much earlier stages was mediated presynaptically by one or both types of channels, two specific antagonists were bath-applied. When exposed to ω-agatoxin TK (100 nM), a specific P/Q-type Ca^{2+} channel blocker, the rhythmic spontaneous activity persisted without significant change in burst parameters (Fig. 5*A*). However, bath application of ω-conotoxin GVIA (300 nM), a specific N-type Ca^{2+} channel blocker, abolished not only the rhythmic spontaneous activity but also the ability of electrical stimulation to evoke bursts ($n = 5$) (Fig. 5*B*). Therefore, our data support the view that N-type Ca^{2+} channels, rather than P/Q-type, mediate the transmitter release responsible for network induced spontaneous bursting in very young chick cords.

Blockade of L-type channels with nifedipine (10 μM) caused only a slight reduction in burst amplitude and duration. However, it inhibited or reduced the accompanying Ca^{2+} transients in most cells, although there were a small number of cells that were only slightly affected. Since these data were derived from cells retrogradely labeled from spinal nerve LS3, the identity of the unaffected cells is unknown (Fig. 5*C*, top). In contrast, blocking P/Q type channels with ω-agatoxin TK was without significant effect on any of the Ca^{2+} transient parameters (Fig. 5*C*, bottom). To determine whether any of the Ca^{2+} during a transient was entering via N-type channels, we directly activated motoneurons with high K^+ (100 mM) to transiently depolarize them to levels required for activation of high voltage-activated channels. In the presence of ω-conotoxin GVIA (300 nM), there was no significant change in mean amplitude or duration of high K^+ evoked Ca^{2+} transients (Fig. 5*C*, bottom).

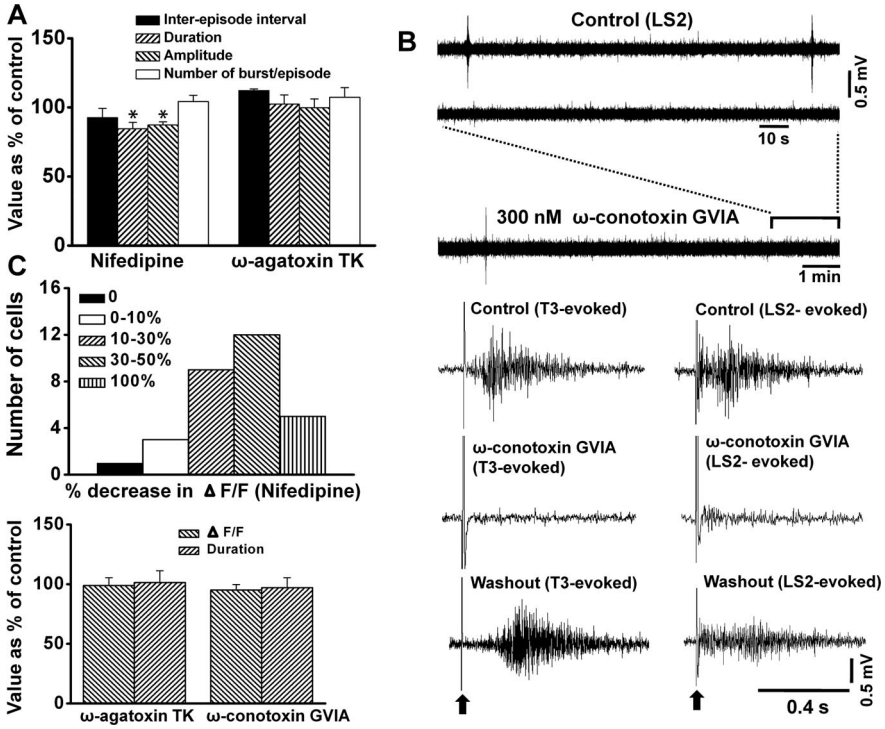

Figure 5. The contribution of high-voltage-activated Ca^{2+} channels to spontaneous bursting episodes and associated Ca^{2+} transients. ***A***, Bar graph showing that the L-type Ca^{2+} blocker nifedipine (10 μM) caused only a modest decrease in burst amplitude and duration ($p < 0.05$) and did not alter interepisode intervals ($p > 0.05$; $n = 6$). Data were derived from femorotibialis, sartorius, and adductor motoneurons and from unidentified motoneurons labeled from spinal nerve LS1. The P/Q-type Ca^{2+} channel blocker ω-agatoxin TK (100 nM) did not alter any burst parameters ($p > 0.05$; $n = 3$). Data were derived from adductor and femorotibialis motoneurons and from those labeled from spinal nerve LS1. ***B***, Top, The N-type Ca^{2+} channel blocker ω-conotoxin GVIA (300 nM) completely blocked spontaneous bursts recorded from spinal nerve LS2. Bottom, In the presence of ω-conotoxin GVIA (300 nM) bursts could not be evoked by activating thoracic segment 3 or by direct stimulation of the cord at LS2 (middle traces) as was possible before drug application (top traces) or after drug washout (bottom traces). The black arrows show stimulus artifact. ***C***, Top bar graph, The numbers of cells labeled from spinal nerve LS3 ($n = 30$) in which nifedipine reduced the amplitude of the Ca^{2+} transients by the percentage indicated. Nifedipine had variable effects on spontaneous Ca^{2+} transients strongly inhibiting many cells but having little effect on others. Bottom bar graph, ω-Agatoxin TK (100 nM) had no effect on the spontaneous Ca^{2+} transients ($p > 0.05$; $n = 7$). ω-Conotoxin GVIA (300 nM) did not alter the mean amplitude or duration of Ca^{2+} transients ($p > 0.05$; $n = 9$) evoked by direct depolarization via 1 min bath application of Tyrode's containing 100 mM KCl. Motoneurons were labeled from spinal nerve LS3. $^*p < 0.05$, $^{**}p < 0.01$ drug treatment versus control. Error bars indicate SEM.

Thus, L-type channels provide much of the intracellular Ca^{2+} responsible for the rhythmic spontaneous Ca^{2+} transients in the soma and the subsequent activation of downstream signaling pathways. In contrast, P/Q-type channels, which are expressed by motoneurons and mediate peripheral neuromuscular transmission, did not contribute. Blocking N-type Ca^{2+} channels prevented spontaneous bursting activity as well as the activation of the network by exogenous stimulation (Fig. 5*B*). This demonstrates that most of the transmitter release responsible for the network activity driving propagating bursts is attributable to N-type channels.

T-type Ca^{2+} channels are activated by relatively small depolarizations and generate low-threshold Ca^{2+} spikes, which can in turn activate Na^+-dependent action potentials and high-voltage-activated Ca^{2+} channels (Perez-Reyes, 2003). T-type channels can also contribute to the generation of spontaneous firing, including bursts, in central neurons (Chevalier et al., 2006; Yaari et al., 2007). T-type currents were previously shown to be present in dissociated E4.5 chick motoneurons (St 24–25), but they declined and became undetectable by E11 (McCobb et al., 1989). We found that blocking T-type channels with 100 μM $NiCl_2$ completely abolished rhythmic spontaneous activity (Fig. 6*A*) in very young cords (St 24 to early St 25; $n = 8$). In addition $NiCl_2$ greatly reduced the asynchronous firing of single motoneurons that occurs spontaneously between bursts (9 ± 1 unit events/min in control vs 1 ± 1 unit events/min in $NiCl_2$) (Fig. 6*A*). Since motoneurons provide the main excitatory drive to reach threshold for network burst initiation, especially at young stages (Hanson and Landmesser, 2003; Arai et al., 2007; O'Donovan et al., 2008), it would be expected that blockade of T-type channels would block spontaneous bursts.

However, it was interesting to note that our ability to elicit bursts in lumbar motoneurons, by propagation of bursts arising from thoracic cord stimulation, was also severely impaired. Bursts were either blocked or only a small number of motoneurons were activated (Fig. 6*B*). We also noticed that the response latency was greatly shortened. The long latency of control bursts after thoracic stimulation indicates a propagation rate of ~10 μm/ms, which is as least 10 times slower than the estimated conduction velocity of even 1 μm unmyelinated axons. Similar rates of propagation were detected with optical imaging of propagating bursts in E8 chick cords (O'Donovan et al., 2008) and suggest

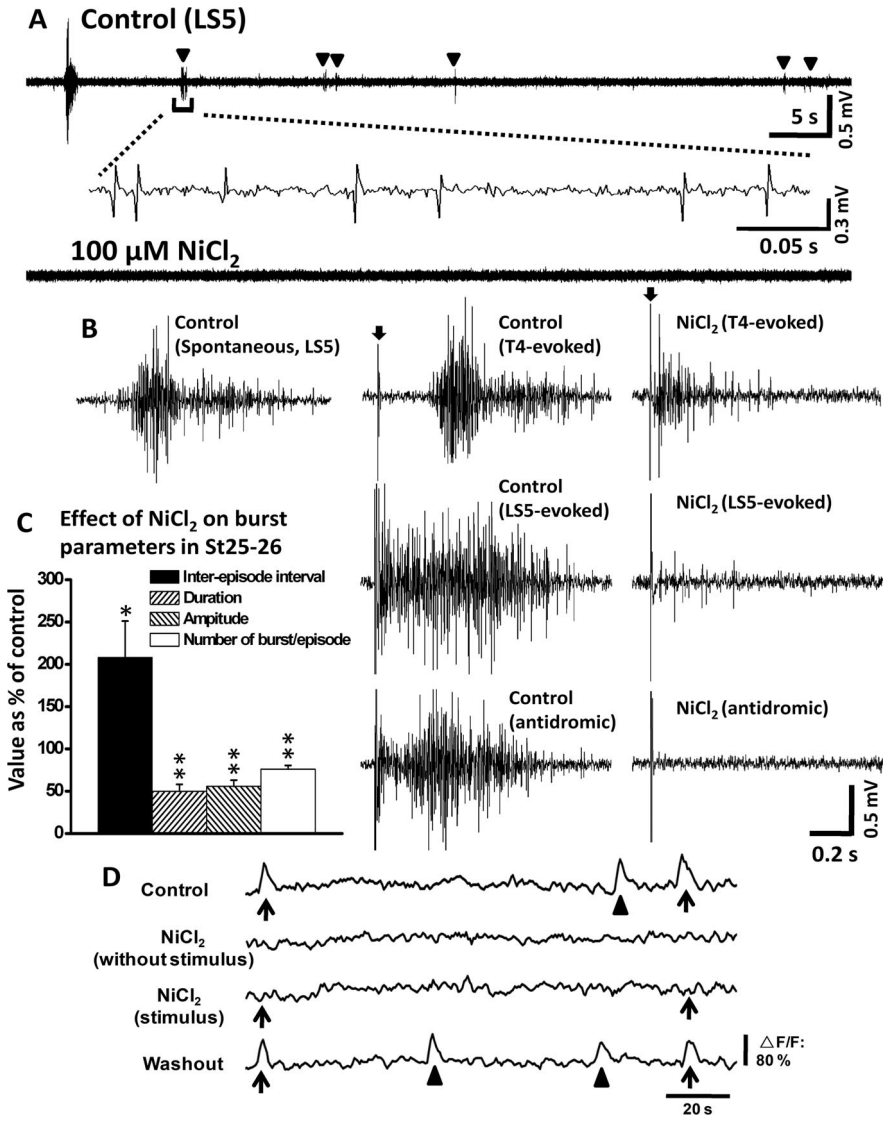

Figure 6. A $NiCl_2$-sensitive Ca^{2+} channel makes a major contribution to the generation of spontaneous bursts and Ca^{2+} transients at early developmental stages. ***A***, $NiCl_2$ (100 μM), which blocks low-voltage-activated T-type channels, completely blocked spontaneous bursting activity in St 24 to early St 25 cords as shown by the example recorded from spinal nerve LS5. The expanded time base below shows the asynchronous firing of single motoneurons between bursting episodes, which was also blocked by $NiCl_2$. ***B***, In controls, bursts could be elicited by electrical stimulation at thoracic cord level T4, by direct stimulation at the cord at LS5, or by antidromic stimulation from the LS5 spinal nerve. However, in the presence of $NiCl_2$, bursts were either blocked or considerably reduced in duration and amplitude after stimulation at T4 or LS5; antidromic stimulation also failed to elicit a burst ($n = 3$). The black arrows indicate stimulus artifact. ***C***, Bar graph showing that 100 μM $NiCl_2$ did not block spontaneous bursting at slightly later stages (late St 25–26), but significantly increased interepisode interval ($p < 0.05$; $n = 10$) and decreased burst duration, amplitude, and the number of burst per episode ($p < 0.01$ for all). Data were derived from sartorius, femorotibialis, and adductor pools. ***D***, Ca^{2+} transients recorded at the level of LS3 from a St 25 embryo. $NiCl_2$ (100 μM) blocked not only spontaneous (arrowheads) but also Ca^{2+} transients evoked (arrows) by thoracic cord stimulation. The effect was reversible with both spontaneous and evoked transients returning after washout of $NiCl_2$. $*p < 0.05$, $**p < 0.01$ treatment versus control. Error bars indicate SEM.

that activity propagates by sequential activation of the network via chemical transmission. When this is blocked by $NiCl_2$, the shorter latency but greatly reduced burst we observed may result from activation of descending fibers that can directly activate some motoneurons. $NiCl_2$ also greatly reduced bursts in response to antidromic activation of motoneurons or to direct stimulation of the cord segments containing the motoneurons (Fig. 6*B*). $NiCl_2$ failed to block spontaneous episodes at slightly later stages (late St 25–26), but significantly increased the interepisode interval and greatly reduced burst amplitude and duration (Fig. 6*C*). Since these parameters were affected similarly in the adductor, sartorius, and femorotibialis pools, the data from all have been combined in Figure 6*C* and expressed as a percentage of the control value.

These observations suggest a critical role of T-type channels in very young spinal cord networks in providing sufficient depolarization to trigger network bursts. However, since 100 μM $NiCl_2$ might also block some R-type channels (Tottene et al., 2000; Gasparini et al., 2001; Su et al., 2002), we treated cords with 100 nM SNX-482, a specific R-type Ca^{2+} channel blocker. This had no effect on spontaneous bursting (data not shown), but since SNX-482 blocks some but not all R-type channels we cannot exclude some contribution of R-type channels. Nevertheless, our results suggest an essential role for $NiCl_2$-sensitive low-voltage-activated channels, probably T-type, in the generation of early spontaneous network activity.

Application of 100 μM $NiCl_2$ (Fig. 6*D*) blocked spontaneous Ca^{2+} transients as well as those in response to exogenous electrical stimulation at T4. However, on washout of $NiCl_2$, spontaneous and evoked Ca^{2+} transients returned ($n = 22$ cells). It is likely that evoked Ca^{2+} transients were blocked because $NiCl_2$ prevented normal size evoked bursts from propagating into the lumber cord. In many cases, only a small number of motoneurons were activated and the level of activation was likely to be below detection for a Ca^{2+} transient. Supporting this idea, we were able to detect asynchronized firing of single action potentials by motoneurons between bursts (Fig. 6*A*), but did not detect any associated Ca^{2+} transients. These observations suggest that we are unable to detect the increased Ca^{2+} resulting from a single motoneuron action potential.

To confirm that T-type currents made an important contribution to the overall Ca^{2+} current, we used patch-clamp recordings from St 27–29 dissociated femorotibialis and sartorius neurons, identified by retrograde labeling with DiI, to characterize the proportion of the total Ca^{2+} current carried by the major Ca^{2+} channel subtypes. Currents in response to voltage steps were recorded in cells exposed to a cumulative sequence of drugs to block the major Ca^{2+} channel subtypes (for details, see Materials and Methods). The recordings (Fig. 7*A–C*) revealed that the current blocked by either 100 μM Ni^{2+} (data not shown) or 2 μM La^{3+} accounted for 62% of the total Ca^{2+} current in femorotibialis motoneurons and 49% in sartorius motoneurons. This is likely to be carried by T-type channels, although because of limitations in drug specificity we cannot exclude a contribution from R-type channels as well. In contrast, L-type channels ac-

counted for only 30% of the Ca^{2+} currents in both types of motoneurons, with N-type channels making even less of a contribution. We also observed that total Ca^{2+} current in sartorius neurons inactivated more rapidly than those in femorotibialis neurons. Thus, low-voltage-activated, $NiCl_2$-sensitive currents, probably T-type, make the greatest contribution to overall Ca^{2+} influx at these early developmental stages.

Persistent Na^+ currents are required for normal levels of spontaneous bursting activity in St 25 spinal cords

Persistent Na^+ currents (I_{NaP}) are important in modulating mammalian motoneuron bursting in mature locomotor circuits (Theiss et al., 2007), and I_{NaP} also contributes to locomotor pattern generation in isolated neonatal rat cords (Tazerart et al., 2007; Zhong et al., 2007; Tazerart et al., 2008; Ziskind-Conhaim et al., 2008). Inhibition of I_{NaP} with riluzole also suppresses spontaneous bursting in disinhibited long term cultures from E14 rat cords (Darbon et al., 2004; Ziskind-Conhaim et al., 2008). However, it was not known whether this current was required for spontaneous activity in intact St 25 chick cords. We found that 10 μM riluzole completely blocked spontaneous activity in four St 25 cords (data not shown). In seven other cords (St 24–27), it did not block activity but significantly increased the interepisode intervals (Fig. 7*D*). Together, our data show that both I_{NaP} and T-type Ca^{2+} channels are required for generating normal levels of spontaneous rhythmic activity during early stages when motoneurons are making important pathfinding decisions.

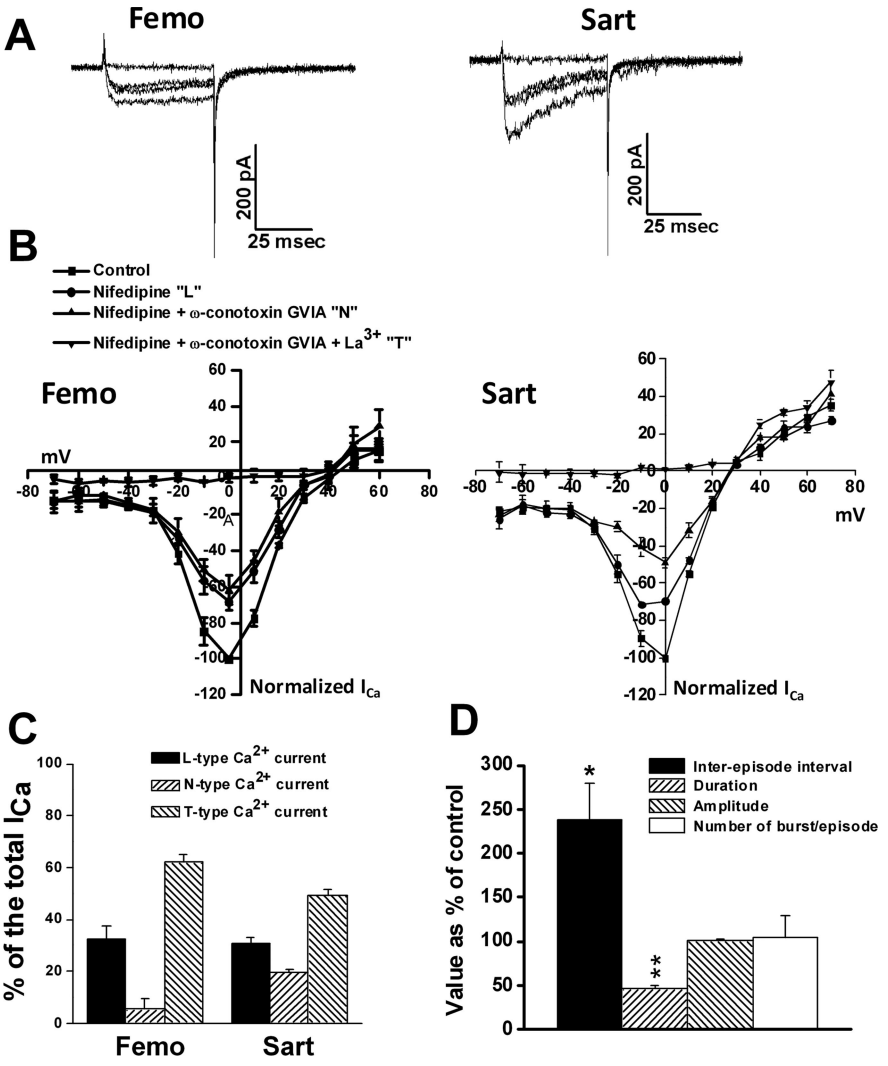

Figure 7. Contribution of different Ca^{2+} channels to motoneuron Ca^{2+} transients at St 27–29 and a persistent sodium current to spontaneous bursting activity. ***A***, Traces are examples (taken from *I–V* plots below) of Ca^{2+} currents in femorotibialis and sartorius motoneurons in response to step depolarizations while the cells were treated with a cumulative sequence of Ca^{2+} channel blockers (see Materials and Methods). ***B***, Comparison of normalized peak current–voltage curves obtained by depolarizing from −120 to +20 mV in 10 mV steps in the presence of different Ca^{2+} current blockers. Nifedipine (5 μM), ω-conotoxin GVIA (1 μM), and La^{3+} (2 μM) were used to block L-, N-, and T-type Ca^{2+} currents, respectively. ***C***, Bar chart compares the proportion of the total Ca^{2+} current carried by each channel subtype. ***D***, The effect of the persistent Na^+ current blocker riluzole on spontaneous bursting activity. Femo, Femorotibialis; Sart, sartorius. $*p < 0.05$, $**p < 0.01$ treatment versus control. Error bars indicate SEM.

The effect of Ca^{2+} release from internal stores on spontaneous bursting and Ca^{2+} transients

To determine whether release of Ca^{2+} from internal stores affected spontaneous bursting or the associated Ca^{2+} transients, we treated cords with 10 μM CPA, to deplete Ca^{2+} from internal stores. This significantly increased the interepisode interval and moderately decreased burst duration, but did not significantly alter burst amplitude or the number of bursts per episode (Fig. 8*A*). CPA also increased the intervals between Ca^{2+} transients and slightly reduced their amplitude (Fig. 8*B*). To test whether the release of Ca^{2+} from ryanodine-sensitive stores affected bursting activity, the antagonist dantrolene (30 μM) was bath applied and was without effect on any burst parameter ($n = 3$) (data not shown). To avoid contaminating the two-photon perfusion system with the colored dantrolene solution, ryanodine was used instead to block Ca^{2+} release from ryanodine-sensitive stores during the imaging of Ca^{2+} transients. Ryanodine (20 μM) produced a slight reduction in Ca^{2+} transient amplitude, similar to that observed with CPA (Fig. 8*B*).

We attempted to assess the importance of Ca^{2+} release via IP_3 receptors. However, the IP_3-sensitive store inhibitor 2-APB also blocks gap junctions (Juszczak and Swiergiel, 2009), which are required for spontaneous bursting (Milner and Landmesser, 1999). Since more selective IP_3 receptor blockers that would be effective in intact cords were unavailable, we applied 10 μM U73122, an inhibitor of phospholipase C. This drug should inhibit production of IP_3 and thus IP_3-mediated release of Ca^{2+} from internal stores. However, it had no effect on burst parameters (Fig. 8*A*) or on the amplitude or duration of Ca^{2+} transients (Fig. 8*B*). Together, our results show that release of Ca^{2+} from internal stores makes only a modest contribution to the spontaneous Ca^{2+} transients in chick motoneurons at these early developmental stages. The effects that were observed appeared to be mediated by ryanodine receptor rather than IP_3 receptor-mediated release.

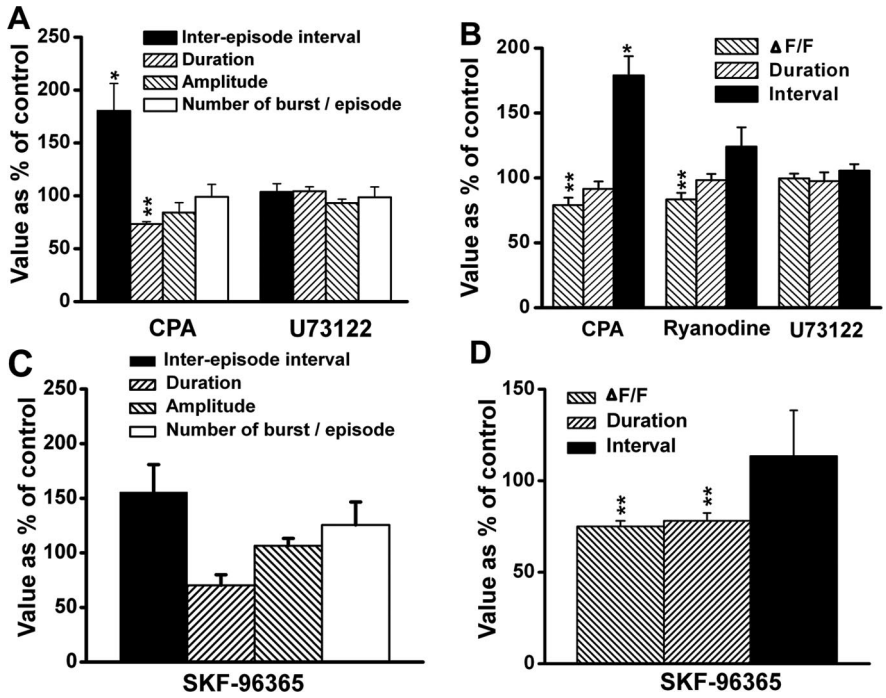

Figure 8. Effect of altering release of Ca^{2+} from internal stores or blocking TRP channels on spontaneous bursts and Ca^{2+} transients. ***A***, CPA (10 μM), which depletes internal stores, significantly increased interepisode intervals ($n = 5$) and decreased the duration of the bursts modestly. U73122 (10 μM), an inhibitor of phospholipase C, had no effect on burst parameters ($p > 0.05$; $n = 5$). ***B***, CPA also increased the intervals and moderately reduced the mean amplitude of the Ca^{2+} transients ($n = 13$). Ryanodine (20 μM) also moderately decreased the mean amplitude of the transients ($n = 17$). Application of U73122 was without effect on Ca^{2+} transient parameters ($n = 9$). ***C***, Bar graph showing that SKF-96365 (10 μM), which blocks some subtypes of TRP channels, had no effect on burst parameters ($n = 5$). ***D***, Bar graph showing that SKF-96365 significantly decreased the mean amplitude and duration of the Ca^{2+} transients ($n = 21$). $^*p < 0.05$, $^{**}p < 0.01$ treatment versus control. Error bars indicate SEM.

Since TRP channels are present on young *Xenopus* spinal neurons and are required to mediate growth cone turning toward chemoattractants in culture (Li et al., 2005b; Wang and Poo, 2005; Jacques-Fricke et al., 2006), we assessed whether relatively selective TRP channel blockers would affect spontaneous bursts and the associated Ca^{2+} transients. SKF-96365 (10 μM), a blocker of a subset of TRP channels (Peña and Ordaz, 2008), tended to increase the intervals between bursting episodes and Ca^{2+} transients but not significantly (Fig. 8*C*). However, SKF-96365 significantly reduced the amplitude and the duration of the Ca^{2+} transients by ~20% (Fig. 8*D*). Although the identification of the channel subtypes is unknown, our results suggest that TRP channels contribute to the excitation that drives spontaneous bursting activity in young spinal cords and that they make a modest contribution to Ca^{2+} transients.

Discussion

We found that the rhythmic spontaneous bursting episodes described previously (Milner and Landmesser, 1999) evoke Ca^{2+} transients in very young lumbar motoneurons, when their somas are still close to the ependymal layer and while they are making pathfinding decisions at the base of the limb. Signaling from these Ca^{2+} transients could thus potentially affect many early events in spinal motor circuit development, including pathfinding, as implied by our previous studies (Hanson and Landmesser, 2004, 2006).

Spontaneous bursting activity and the associated Ca^{2+} transients are widespread in the developing nervous system. However, the roles of such activity/transients, especially at early stages of circuit formation, are only beginning to be understood. It is important to recognize that these roles, and indeed the underlying mechanisms by which such activity is generated, may also differ between species and at different developmental stages (Spitzer, 2006; Root et al., 2008). Before network-generated activity, different subtypes of *Xenopus* spinal neurons exhibit different Ca^{2+} transient frequencies and these are required to appropriately specify neurotransmitter phenotypes (Borodinsky et al., 2004). The present study showed that the propagating waves of activity in St 25 chick cords produce relatively synchronous Ca^{2+} transients in all motoneurons. Thus, different motoneuron subtypes would be unable to use Ca^{2+} transient frequency differences to drive subtype-specific differences in downstream signaling. However, our previous studies clearly showed that different pathfinding decisions were highly sensitive to modest alterations in the normal frequency, emphasizing the importance of maintaining the normal *in vivo* frequency. Other aspects of early cord circuit formation may also be sensitive to modest alterations in frequency.

Given the strong homeostatic changes that occur in developing cord circuits when activity is perturbed (Chub and O'Donovan, 1998; Milner and Landmesser, 1999; Gonzalez-Islas and Wenner, 2006; Wilhelm et al., 2009), it seems unlikely that complex circuits could form normally in the absence of activity. Birds and placental mammals undergo long periods of development (~3 weeks for chicks and mice, much longer for primates) in the absence of extrinsic sensory stimuli that could activate developing spinal circuits. Thus, spontaneous rhythmic activity may have evolved to supply such activity during this period. Different signaling systems regulating downstream developmental processes may have evolved to be tuned to the normal frequency of this activity. However, despite near-synchronous activation on the minute timescale, we observed that the waves and associated Ca^{2+} transients propagate at speeds of 10 μm/ms. Thus, near neighbors will be more synchronously activated than cells that are farther apart, and, as in the visual system, these differences could be used to drive spike timing-dependent refinement of connections. The window for spike timing plasticity in the intact *Xenopus* tectum (Zhang et al., 1998) is very narrow (~20 ms). Additional studies will be needed to see whether such mechanisms are used in developing spinal circuits and whether they make use of information encoded in the spontaneous waves.

The frequency and pattern of Ca^{2+} transients have been shown to activate different patterns of gene transcription (Dolmetsch et al., 1998) and intracellular signaling pathways (Moody and Bosma, 2005; Greer and Greenberg, 2008). In cultured *Xenopus* spinal neurons GAD 67 expression and thus the GABAergic phenotype is regulated by the frequency of Ca^{2+} transients (Watt et al., 2000). Altering activity in intact spinal cords changed the proportion of neurons that expressed either excitatory or inhibitory neurotransmitters (Spitzer et al., 2004; Root et al., 2008). It will be important to now characterize the intracellular pathways by

which alterations in the frequency of Ca^{2+} transients affected distinct D–V and pool-specific pathfinding decisions. To exclude alterations in GABAergic and glycinergic signaling in contributing to the pathfinding errors, we are using channelrhodopsin 2 (Li et al., 2005a) to alter frequency, independent of drugs that affect neurotransmitters (K. Kastanenka, unpublished observations). Although the Ca^{2+} transients we observed occurred relatively synchronously, they did exhibit pool-specific differences in duration. These differences could be used by downstream effectors to decode information and to generate different pool-specific responses, as was previously shown in lymphocytes (Dolmetsch et al., 1997).

Another interesting finding was that Ca^{2+} transients occurred in some presumed precursor cells in the ependymal layer/germinal epithelium and these were synchronous with the motoneuron Ca^{2+} transients. These were blocked by nicotinic antagonists that blocked the neurally generated activity. It will be important to determine the identity of these ependymal cells and how neural network activity causes Ca^{2+} transients. It will also be interesting to determine whether blocking the transients has any effect on the proliferation or differentiation of cells that generate different subclasses of motoneurons and interneurons. Propagating Ca^{2+} transients have been observed in radial glial cells in the neocortex in which they regulate cell proliferation (Weissman et al., 2004) and in the ventricular zone of the developing rabbit retina, in which they were also dependent on neurally generated waves (Syed et al., 2004).

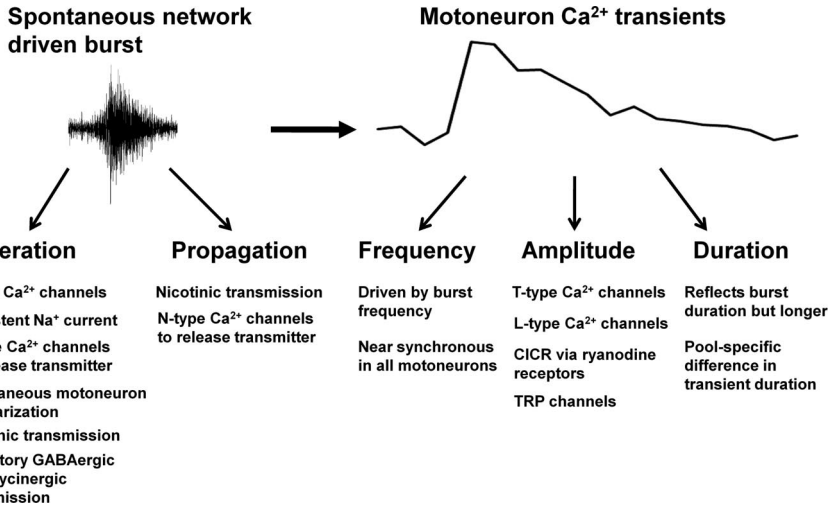

Figure 9. Summary of currents and network mechanisms underlying spontaneous propagating bursting activity and the associated Ca^{2+} transients in St 25 chick cords. Spontaneous bursts of activity are generated by spontaneous motoneuron depolarization and the release of ACh to depolarize other motoneurons and interneurons. To reach the network threshold to generate a propagating burst requires T-type Ca^{2+} channels and a persistent Na^{+} current as well as N-type Ca^{2+} channels to release excitatory transmitters. Although GABA and glycine contribute to the excitatory drive, they are not essential to generate a burst, whereas ACh is required. Propagation of the bursts requires N-type Ca^{2+} channels to release excitatory transmitters and nicotinic transmission. Although bursts can be elicited by exogenous stimulation during nicotinic blockade, nicotinic transmission is what normally drives bursting. The depolarization of the motoneurons during the bursts causes Ca^{2+} transients. Their frequency is driven by the burst frequency and is near synchronous in all motoneurons. The amplitude of the Ca^{2+} transients is determined by Ca^{2+} coming from different sources. The greatest contribution is via L-type and T-type Ca^{2+} channels, with a lesser contribution from N-type. Calcium-induced calcium release from internal stores makes only a modest contribution and this is mediated by ryanodine-sensitive receptors rather than IP_3. TRP channels also make a modest contribution. Pool-specific differences in transient duration were observed, and these reflect pool-specific difference in burst duration, only longer.

Neurotransmitters released during propagating bursts could also affect Ca^{2+} transients. As noted above, blocking $GABA_A$ receptors did not affect transient duration or amplitude and blockade of metabotropic $GABA_B$ receptors was without effect on any transient parameter. Nicotinic transmission and signaling via a variety of receptor subtypes, including $\alpha7$ and $\alpha4\beta2$, play important roles in neural development (Pugh and Berg, 1994; McLaughlin et al., 2003; Myers et al., 2005; Liu et al., 2006). However, although $\alpha7$ receptors have a high Ca^{2+} permeability and can mediate transmission in ciliary neurons (Zhang et al., 1996; Ullian et al., 1997; Sargent, 2009), we found that blocking them had little effect on bursting episodes or Ca^{2+} transients. In contrast, blocking either $\alpha4\beta2$ receptors with DHβE or $\alpha3\beta4$ receptors with mecamylamine both transiently blocked spontaneous bursting. However, these drugs did not affect the amplitude or duration of Ca^{2+} transients evoked in sartorius or femorotibialis neurons during nicotinic blockade. Since we were able to elicit propagating bursts via electrical stimulation during the period of blockade with either antagonist, these receptors also are not essential for bursts to propagate. However, ACh acting on them is what normally drives bursting activity. One possibility is that the waves evoked during blockade with these antagonists are driven by other neurotransmitters (Milner and Landmesser, 1999); alternatively, ACh released by exogenous stimulation may act on other nicotinic receptor subtypes.

A major contribution of the present study was to characterize the sources of the Ca^{2+} that mediate bursts and their associated Ca^{2+} transients. These and the relationship between different currents, propagating bursts, and the Ca^{2+} transients are summarized in Figure 9. A $NiCl_2$-sensitive low-voltage-activated Ca^{2+} current, probably T-type, as well as a persistent Na^{+} current was essential for the generation of spontaneous activity at these early stages. The main contribution to intracellular Ca^{2+} associated with the bursts was Ca^{2+} influx via T-type and L-type channels rather than N-type or P/Q-type. Although blocking P/Q- or L-type channels had negligible effects on bursting activity, blocking N-type channels completely prevented bursting activity even with exogenous stimulation. This appeared to be because N-type channels mediate the release of the neurotransmitters required to initiate network driven bursts. This observation emphasizes the importance of chemical transmission in this process. Finally, we found that TRP-like channels and ryanodine-sensitive Ca^{2+} stores also made a modest contribution to the Ca^{2+} transients.

Voltage-dependent Ca^{2+} channels were the main contributors to the Ca^{2+} transients that we observed, with L-type channels making a major contribution, as shown previously at later stages in both rat (Scamps et al., 1998; Dayanithi et al., 2006) and chick (McCobb et al., 1989) dissociated motoneurons. Although L-type channels were not essential for spontaneous bursting, they may mediate downstream signaling events. We found that release from internal Ca^{2+} stores made only a modest contribution to the transients, which differs from the Ca^{2+} transients in *Xenopus* cords at earlier developmental stages. The release we observed was via ryanodine-sensitive receptors similar to observations made in older rat motoneurons (Dayanithi et al., 2006).

T-type currents were previously shown to be important for the generation of spontaneous Ca^{2+} transients in *Xenopus* mo-

toneurons (Gu and Spitzer, 1993; Gu et al., 1994). However, such currents had not been shown to be essential for propagating wave-like activity in either the retina or spinal cord. We found that a $NiCl_2$-sensitive current, probably T-type, was essential not only for the generation of spontaneous bursting activity, but also for the propagating spread of excitation via network-mediated neurotransmission. Given that waves of activity at this stage appear to originate predominately in the upper cervical cord (Momose-Sato et al., 2009), excitation mediated by T-type channels would be essential for the normal bursting activity and Ca^{2+} transients experienced by lumbar motoneurons *in ovo*. A second novel observation was that a riluzole-sensitive I_{NaP} was also essential for the generation of normal levels of spontaneous activity at these early stages. Although known to be important for the activation of locomotor patterns in neonatal mammalian cords in response to neuromodulators (Tazerart et al., 2007; Zhong et al., 2007; Ziskind-Conhaim et al., 2008), I_{NaP} was not previously implicated in the generation of spontaneous rhythmic activity in young cord circuits.

Together, our findings offer insights into the features of spinal motor circuits that mediate rhythmic spontaneous bursting activity and Ca^{2+} transients in very young chick spinal cords. It will now be important to determine how the precise frequency of Ca^{2+} transients is read out to influence both the dorsal–ventral and pool-specific pathfinding decisions made by embryonic motoneurons and how early other spinal neuron subtypes (Goulding and Pfaff, 2005) exhibit Ca^{2+} transients and thus come under their potential influence.

References

Arai Y, Mentis GZ, Wu JY, O'Donovan MJ (2007) Ventrolateral origin of each cycle of rhythmic activity generated by the spinal cord of the chick embryo. PLoS One 2:e417.

Berridge MJ, Bootman MD, Roderick HL (2003) Calcium signalling: dynamics, homeostasis and remodelling. Nat Rev Mol Cell Biol 4:517–529.

Bertrand D, Galzi JL, Devillers-Thiéry A, Bertrand S, Changeux JP (1993) Mutations at two distinct sites within the channel domain M2 alter calcium permeability of neuronal alpha 7 nicotinic receptor. Proc Natl Acad Sci U S A 90:6971–6975.

Bootman MD, Collins TJ, Peppiatt CM, Prothero LS, MacKenzie L, De Smet P, Travers M, Tovey SC, Seo JT, Berridge MJ, Ciccolini F, Lipp P (2001) Calcium signalling—an overview. Semin Cell Dev Biol 12:3–10.

Borodinsky LN, Root CM, Cronin JA, Sann SB, Gu X, Spitzer NC (2004) Activity-dependent homeostatic specification of transmitter expression in embryonic neurons. Nature 429:523–530.

Branchereau P, Morin D, Bonnot A, Ballion B, Chapron J, Viala D (2000) Development of lumbar rhythmic networks: from embryonic to neonate locomotor-like patterns in the mouse. Brain Res Bull 53:711–718.

Cang J, Rentería RC, Kaneko M, Liu X, Copenhagen DR, Stryker MP (2005) Development of precise maps in visual cortex requires patterned spontaneous activity in the retina. Neuron 48:797–809.

Chandrasekaran AR, Plas DT, Gonzalez E, Crair MC (2005) Evidence for an instructive role of retinal activity in retinotopic map refinement in the superior colliculus of the mouse. J Neurosci 25:6929–6938.

Chevalier M, Lory P, Mironneau C, Macrez N, Quignard JF (2006) T-type CaV3.3 calcium channels produce spontaneous low-threshold action potentials and intracellular calcium oscillations. Eur J Neurosci 23:2321–2329.

Chub N, O'Donovan MJ (1998) Blockade and recovery of spontaneous rhythmic activity after application of neurotranmitter antagonists to spinal networks of the chick embryo. J Neurosci 18:294–306.

Clapham DE (2007) Calcium signaling. Cell 131:1047–1058.

Darbon P, Yvon C, Legrand JC, Streit J (2004) I_{NaP} underlies intrinsic spiking and rhythm generation in networks of cultured rat spinal cord neurons. Eur J Neurosci 20:976–988.

Dayanithi G, Mechaly I, Viero C, Aptel H, Alphandery S, Puech S, Bancel F, Valmier J (2006) Intracellular Ca^{2+} regulation in rat motoneurons during development. Cell Calcium 39:237–246.

Dolmetsch RE, Lewis RS, Goodnow CC, Healy JI (1997) Differential activation of transcription factors induced by Ca^{2+} response amplitude and duration. Nature 386:855–858.

Dolmetsch RE, Xu K, Lewis RS (1998) Calcium oscillations increase the efficiency and specificity of gene expression. Nature 392:933–936.

Fedirchuk B, Wenner P, Whelan PJ, Ho S, Tabak J, O'Donovan MJ (1999) Spontaneous network activity transiently depresses synaptic transmission in the embryonic chick spinal cord. J Neurosci 19:2102–2112.

Gasparini S, Kasyanov AM, Pietrobon D, Voronin LL, Cherubini E (2001) Presynaptic R-type calcium channels contribute to fast excitatory synaptic transmission in the rat hippocampus. J Neurosci 21:8715–8721.

Gonzalez-Islas C, Wenner P (2006) Spontaneous network activity in the embryonic spinal cord regulates AMPAergic and GABAergic synaptic strength. Neuron 49:563–575.

Goulding M, Pfaff SL (2005) Development of circuits that generate simple rhythmic behaviors in vertebrates. Curr Opin Neurobiol 15:14–20.

Greer PL, Greenberg ME (2008) From synapse to nucleus: calcium-dependent gene transcription in the control of synapse development and function. Neuron 59:846–860.

Gu X, Spitzer NC (1993) Low-threshold Ca^{2+} current and its role in spontaneous elevations of intracellular Ca^{2+} in developing *Xenopus* neurons. J Neurosci 13:4936–4948.

Gu X, Olson EC, Spitzer NC (1994) Spontaneous neuronal calcium spikes and waves during early differentiation. J Neurosci 14:6325–6335.

Hanson MG, Landmesser LT (2003) Characterization of the circuits that generate spontaneous episodes of activity in the early embryonic mouse spinal cord. J Neurosci 23:587–600.

Hanson MG, Landmesser LT (2004) Normal patterns of spontaneous activity are required for correct motor axon guidance and the expression of specific guidance molecules. Neuron 43:687–701.

Hanson MG, Landmesser LT (2006) Increasing the frequency of spontaneous rhythmic activity disrupts pool-specific axon fasciculation and pathfinding of embryonic spinal motoneurons. J Neurosci 26:12769–12780.

Hata K, Polo-Parada L, Landmesser LT (2007) Selective targeting of different neural cell adhesion molecule isoforms during motoneuron myotube synapse formation in culture and the switch from an immature to mature form of synaptic vesicle cycling. J Neurosci 27:14481–14493.

Jacques-Fricke BT, Seow Y, Gottlieb PA, Sachs F, Gomez TM (2006) Ca^{2+} influx through mechanosensitive channels inhibits neurite outgrowth in opposition to other influx pathways and release from intracellular stores. J Neurosci 26:5656–5664.

Juszczak GR, Swiergiel AH (2009) Properties of gap junction blockers and their behavioural, cognitive and electrophysiological effects: animal and human studies. Prog Neuropsychopharmacol Biol Psychiatry 33:181–198.

Katz E, Protti DA, Ferro PA, Rosato Siri MD, Uchitel OD (1997) Effects of Ca^{2+} channel blocker neurotoxins on transmitter release and presynaptic currents at the mouse neuromuscular junction. Br J Pharmacol 121:1531–1540.

Keiger CJ, Prevette D, Conroy WG, Oppenheim RW (2003) Developmental expression of nicotinic receptors in the chick and human spinal cord. J Comp Neurol 455:86–99.

Li X, Gutierrez DV, Hanson MG, Han J, Mark MD, Chiel H, Hegemann P, Landmesser LT, Herlitze S (2005a) Fast noninvasive activation and inhibition of neural and network activity by vertebrate rhodopsin and green algae channelrhodopsin. Proc Natl Acad Sci U S A 102:17816–17821.

Li Y, Jia YC, Cui K, Li N, Zheng ZY, Wang YZ, Yuan XB (2005b) Essential role of TRPC channels in the guidance of nerve growth cones by brain-derived neurotrophic factor. Nature 434:894–898.

Liu Z, Neff RA, Berg DK (2006) Sequential interplay of nicotinic and GABAergic signaling guides neuronal development. Science 314:1610–1613.

McCobb DP, Best PM, Beam KG (1989) Development alters the expression of calcium currents in chick limb motoneurons. Neuron 2:1633–1643.

McLaughlin T, Torborg CL, Feller MB, O'Leary DD (2003) Retinotopic map refinement requires spontaneous retinal waves during a brief critical period of development. Neuron 40:1147–1160.

Milner LD, Landmesser LT (1999) Cholinergic and GABAergic inputs drive patterned spontaneous motoneuron activity before target contact. J Neurosci 19:3007–3022.

Mlinar B, Enyeart JJ (1993) Block of current through T-type calcium chan-

nels by trivalent metal cations and nickel in neural rat and human cells. J Physiol 469:639–652.
Momose-Sato Y, Mochida H, Kinoshita M (2009) Origin of the earliest correlated neuronal activity in the chick embryo revealed by optical imaging with voltage-sensitive dyes. Eur J Neurosci 29:1–13.
Moody WJ, Bosma MM (2005) Ion channel development, spontaneous activity, and activity-dependent development in nerve and muscle cells. Physiol Rev 85:883–941.
Myers CP, Lewcock JW, Hanson MG, Gosgnach S, Aimone JB, Gage FH, Lee KF, Landmesser LT, Pfaff SL (2005) Cholinergic input is required during embryonic development to mediate proper assembly of spinal locomotor circuits. Neuron 46:37–49.
Nishimaru H, Iizuka M, Ozaki S, Kudo N (1996) Spontaneous motoneuronal activity mediated by glycine and GABA in the spinal cord of rat fetuses in vitro. J Physiol 497:131–143.
O'Donovan MJ, Bonnot A, Mentis GZ, Arai Y, Chub N, Shneider NA, Wenner P (2008) Imaging the spatiotemporal organization of neural activity in the developing spinal cord. Dev Neurobiol 68:788–803.
Papke RL, Dwoskin LP, Crooks PA, Zheng G, Zhang Z, McIntosh JM, Stokes C (2008) Extending the analysis of nicotinic receptor antagonists with the study of alpha6 nicotinic receptor subunit chimeras. Neuropharmacology 54:1189–1200.
Peña F, Ordaz B (2008) Non-selective cation channel blockers: potential use in nervous system basic research and therapeutics. Mini Rev Med Chem 8:812–819.
Perez-Reyes E (2003) Molecular physiology of low-voltage-activated T-type calcium channels. Physiol Rev 83:117–161.
Protti DA, Uchitel OD (1993) Transmitter release and presynaptic Ca^{2+} currents blocked by the spider toxin omega-Aga-IVA. Neuroreport 5:333–336.
Protti DA, Reisin R, Mackinley TA, Uchitel OD (1996) Calcium channel blockers and transmitter release at the normal human neuromuscular junction. Neurology 46:1391–1396.
Pugh PC, Berg DK (1994) Neuronal acetylcholine receptors that bind alpha-bungarotoxin mediate neurite retraction in a calcium-dependent manner. J Neurosci 14:889–896.
Root CM, Velázquez-Ulloa NA, Monsalve GC, Minakova E, Spitzer NC (2008) Embryonically expressed GABA and glutamate drive electrical activity regulating neurotransmitter specification. J Neurosci 28:4777–4784.
Rusin KI, Moises HC (1995) μ-Opioid receptor activation reduces multiple components of high-threshold calcium current in rat sensory neurons. J Neurosci 15:4315–4327.
Sargent PB (2009) Nicotinic receptors concentrated in the subsynaptic membrane do not contribute significantly to synaptic currents at an embryonic synapse in the chicken ciliary ganglion. J Neurosci 29:3749–3759.
Scamps F, Valentin S, Dayanithi G, Valmier J (1998) Calcium channel subtypes responsible for voltage-gated intracellular calcium elevations in embryonic rat motoneurons. Neuroscience 87:719–730.
Séguéla P, Wadiche J, Dineley-Miller K, Dani JA, Patrick JW (1993) Molecular cloning, functional properties, and distribution of rat brain α7: a nicotinic cation channel highly permeable to calcium. J Neurosci 13:596–604.
Sernagor E, Chub N, Ritter A, O'Donovan MJ (1995) Pharmacological characterization of the rhythmic synaptic drive onto lumbosacral motoneurons in the chick embryo spinal cord. J Neurosci 15:7452–7464.
Spitzer NC (2006) Electrical activity in early neuronal development. Nature 444:707–712.
Spitzer NC, Root CM, Borodinsky LN (2004) Orchestrating neuronal differentiation: patterns of Ca^{2+} spikes specify transmitter choice. Trends Neurosci 27:415–421.
Stellwagen D, Shatz CJ (2002) An instructive role for retinal waves in the development of retinogeniculate connectivity. Neuron 33:357–367.
Su H, Sochivko D, Becker A, Chen J, Jiang Y, Yaari Y, Beck H (2002) Upregulation of a T-type Ca^{2+} channel causes a long-lasting modification of neuronal firing mode after status epilepticus. J Neurosci 22:3645–3655.
Syed MM, Lee S, He S, Zhou ZJ (2004) Spontaneous waves in the ventricular zone of developing mammalian retina. J Neurophysiol 91:1999–2009.
Tazerart S, Viemari JC, Darbon P, Vinay L, Brocard F (2007) Contribution of persistent sodium current to locomotor pattern generation in neonatal rats. J Neurophysiol 98:613–628.
Tazerart S, Vinay L, Brocard F (2008) The persistent sodium current generates pacemaker activities in the central pattern generator for locomotion and regulates the locomotor rhythm. J Neurosci 28:8577–8589.
Theiss RD, Kuo JJ, Heckman CJ (2007) Persistent inward currents in rat ventral horn neurones. J Physiol 580:507–522.
Tottene A, Volsen S, Pietrobon D (2000) α_{1E} subunits form the pore of three cerebellar R-type calcium channels with different pharmacological and permeation properties. J Neurosci 20:171–178.
Tsuchida T, Ensini M, Morton SB, Baldassare M, Edlund T, Jessell TM, Pfaff SL (1994) Topographic organization of embryonic motor neurons defined by expression of LIM homeobox genes. Cell 79:957–970.
Uchitel OD, Protti DA, Sanchez V, Cherksey BD, Sugimori M, Llinás R (1992) P-type voltage-dependent calcium channel mediates presynaptic calcium influx and transmitter release in mammalian synapses. Proc Natl Acad Sci U S A 89:3330–3333.
Ullian EM, McIntosh JM, Sargent PB (1997) Rapid synaptic transmission in the avian ciliary ganglion is mediated by two distinct classes of nicotinic receptors. J Neurosci 17:7210–7219.
Wang GX, Poo MM (2005) Requirement of TRPC channels in netrin-1-induced chemotropic turning of nerve growth cones. Nature 434:898–904.
Watt SD, Gu X, Smith RD, Spitzer NC (2000) Specific frequencies of spontaneous Ca^{2+} transients upregulate GAD 67 transcripts in embryonic spinal neurons. Mol Cell Neurosci 16:376–387.
Weissman TA, Riquelme PA, Ivic L, Flint AC, Kriegstein AR (2004) Calcium waves propagate through radial glial cells and modulate proliferation in the developing neocortex. Neuron 43:647–661.
Wilhelm JC, Rich MM, Wenner P (2009) Compensatory changes in cellular excitability, not synaptic scaling, contribute to homoestatic recovery of embryonic network activity. Proc Natl Acad Sci U S A 106:6760–6765.
Wu GY, Deisseroth K, Tsien RW (2001) Spaced stimuli stabilize MAPK pathway activation and its effects on dendritic morphology. Nat Neurosci 4:151–158.
Yaari Y, Yue C, Su H (2007) Recruitment of apical dendritic T-type Ca^{2+} channels by backpropagating spikes underlies de novo intrinsic bursting in hippocampal epileptogenesis. J Physiol 580:435–450.
Zhang LI, Tao HW, Holt CE, Harris WA, Poo M (1998) A critical window for cooperation and competition among developing retinotectal synapses. Nature 395:37–44.
Zhang ZW, Coggan JS, Berg DK (1996) Synaptic currents generated by neuronal acetylcholine receptors sensitive to alpha-bungarotoxin. Neuron 17:1231–1240.
Zhong G, Masino MA, Harris-Warrick RM (2007) Persistent sodium currents participate in fictive locomotion generation in neonatal mouse spinal cord. J Neurosci 27:4507–4518.
Ziskind-Conhaim L, Wu L, Wiesner EP (2008) Persistent sodium current contributes to induced voltage oscillations in locomotor-related hb9 interneurons in the mouse spinal cord. J Neurophysiol 100:2254–2264.